DOI: 10.3126/hijost.v8i1.83091

RESEARCH ARTICLE

Himalayan Journal of Science and Technology

Volume 8: 1201 (2024)

First-Principles Calculations to Investigate Structural, Spectroscopic Features, Electronic and Thermodynamic Properties of Trichloroacetaldehyde

Bishwo Basnet, Abhishek Rana Magar, Rabin Ghimire, Usha Joshi, Krishna Bahadur Rai*

Department of Physics, Patan Multiple Campus, Tribhuvan University, Nepal

ARTICLE INFO

Article History
Received: 9 November 2024
Accepted: 15 May 2025

Keywords:
Trichloroacetaldehyde
Density functional theory
Vibrational analysis
HOMO-LUMO
Density of state
Thermodynamic properties

Correspondence
Krishna Bahadur Rai
e-mail: krishna.rai@pmc.tu.edu.np

ABSTRACT

Trichloroacetaldehyde is an oily liquid which has pungent smell with irritating odor. DFT with B3LYP/6-311++G (d, p) basis set together with Gauss Sum 3.0.2 and Moltran software were used to study this molecule. The molecule's optimization energy was found to be -41707.52 eV. From the FT-IR spectroscopy, the C-H stretching vibration are observed at 2974 cm^{-1}. The C=O stretching, C–H stretching, C–Cl stretching, C–H bending vibrations are also seen at various spectrum modes. The molecular electrostatic potential and electrostatic potential have shown that the region near oxygen has highest electrophilic activity and the region near hydrogen has the highest nucleophilic activity. The electrostatic potential on to the surface with electron density allows visualization of the molecule's size, shape, charge density and reactive sites. HOMO-LUMO energy gap has a significant stability index and its value is 5.99 eV. Density of states (DOS) allows us to stimulate electrons moving from the valence band into the conduction band and its value is 6.01 eV and is very much close to energy gap (5.99 eV) obtained from HOMO-LUMO gap. The global reactivity parameter i.e. hardness is 2.99 eV, softness is 0.33 eV^{-1}, chemical potential is -5.47 eV, electronegativity is 5.47 eV and electrophilicity index is 5.00 eV, has been observed. Mulliken atomic charges analysis shows that atoms Cl2, Cl3, Cl4 and C5 along with O7 have negative charges and C1 and H6 atoms contain positive charge. The thermodynamic parameters i.e. heat capacity at constant volume, heat capacity at constant pressure, internal energy, enthalpy and entropy increase except Gibb's free energy with rise in temperature.

1. INTRODUCTION

Trichloroacetaldehyde, also known as chloral, is an oily liquid characterized by a sharp, pungent odor that can be irritating. Its chemical formula is Cl_3CCHO. It has a melting point of -57.5 °C and a boiling point of 97.8 °C. At 20 °C, its density is 1.51 gcm^{-3}, compared to H_2O at 4°C. Figure 1 shows the chemical structure of trichloroacetaldehyde in which two carbon atoms are joined to other elements by covalent bonds in the structure of it. When three hydrogen atoms of acetaldehyde are replaced by three chlorine atoms, trichloroacetaldehyde is formed. Another carbon atom forms a single bond with one hydrogen atom and a double bond with one oxygen atom (Gordeev et al., 1996). It may be readily dissolved in water to form chloral hydrate, which is soluble in ethanol and diethyl ether. In the presence of sulfuric acid and light, it polymerizes to form meta-chloral, a white solid trimer (Abbas et al., 1997). Chlorine and naturally occurring organic material react to generate chloral hydrate, which is trichloroacetaldehyde in hydrated form. This reaction occurs during the water treatment process (Barrott, 2004). The chloral molecule contains two functional groups, carbonyl and trichloromethyl, which together activate the molecule and increase its synthetic potential as a dual-reactive chemical. It can be changed into derivatives of formyl and dichlorovinyl (Luknitskii, 1975). Acetaldehyde is the simple form of aldehyde which has a poisonous and extremely reactive character. Aldehyde is

categorized as a class 1 toxin (human carcinogen). Alcohol consumption is the primary source of acetaldehyde (Rajendram et al., 2016). Reactive oxygen species (ROS) caused cells to undergo apoptosis as a result of the damage to the mitochondria. If alcohol consumption is removed efficiently, it may eliminate volume of acetaldehyde and prevents cellular toxicity (Li et al., 2018). The lowest stable energy value for formaldehyde, acetaldehyde, formamide and acrolein seems 114.54, 153.88, 169.95, and 191.97 Hartree respectively together with their respective HOMO-LUMO gap are 0.21 eV, 0.22 eV, 0.10 eV, and 0.29 eV from the DFT calculaton. Moreover, the aldehyde family exhibits peaks for the stretching vibration between C-H and C=O (Limbu et al., 2024).

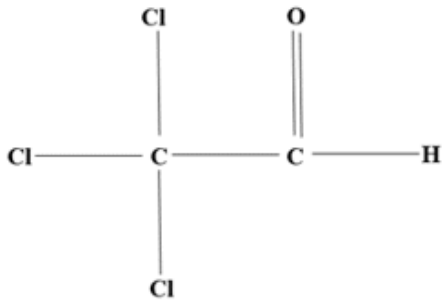

Figure 1
Chemical structure of trichloroacetaldehyde

In recent years, several research articles about trichloroacetaldehyde have been published. Using measurements of solar flux intensity from the spectro-radiometer, researchers examined the photochemical degradation of chloral and found the maximum loss rate of chloral (Neupane et al., 2022; Nolan et al., 2002). In 2016, O'Nolan et al., studied the crystallographic parameters of chloral hydrate and its betaine cocrystal as well as its polymorphs (O'Nolan et al., 2016). The modification of trichloroacetaldehyde oligonucleotides by Gaus et al., offered that the producing oligonucleotides of superior quality requires not only a deep comprehension of the manufacturing process but also a careful examination and management of the raw material supply chain (Gaus et al., 2005). However, equilibrium configuration, spectroscopic vibrational analysis, electronic structures and thermodynamics properties of trichloroacetaldehyde have never been performed before using the first principles density functional theory (DFT) calculation. So, this study is essential and important to get deep understanding of molecular behavior of optimized structure, vibration analysis, molecular electrostatics potential (MEP), electrostatic potential (ESP), electron density (ED), highest occupied molecular orbital-lowest unoccupied molecular orbital (HOMO-LUMO) energy gap, density of states (DOS), global reactivity descriptors, Mulliken atomic charges and thermodynamic properties of trichloroacetaldehyde using DFT with B3LYP/6-311++G (d, p) basis set together with Gauss Sum 3.0.2 and Moltran software. In this study, 6-311++G (d, p) is 6-311G basis set with added d-polarization functions on non-hydrogen atoms and p polarizations for hydrogen.

2. COMPUTATIONAL METHODOLOGY

The computations of the trichloroacetaldehyde molecules were completed using the Gaussian09W (Frisch et al., 2009) program and Gauss View 6.0 (Frisch et al., 2000) interface. DFT/B3LYP approach with 6-311++G (d, p) (Becke et al., 1996) basis set was used to generate the optimized structure, optimization energy, FT-IR spectra, MEP, ESP, ED, HOMO-LUMO energy gap and Mulliken atomic charges. For finding these different representations and different outcomes, the .log and .chk files produced using the Gaussian DFT were utilized. Gauss Sum 3.0.2 software was used as supplementary software to get the DOS spectra. The necessary data for the thermodynamics properties such as heat capacity at constant volume (C_v) and constant pressure (C_p), internal energy (U), enthalpy (H), entropy (S) and Gibbs free energy (G) were obtained using the Moltran software (Ignatov, 2015). Origin Pro 9.0 software (Edwards et al., 2002) was used to plot the data and for its analysis.
Ionization potential (I) and electron affinity (A) are directly correlated with HOMO and LUMO energy respectively and this ionization potential (I) and electron affinity (A) are

$$I = -E_{HOMO} \quad \ldots\ldots\ldots\ldots (1)$$
$$A = -E_{LUMO} \quad \ldots\ldots\ldots\ldots (2)$$

Koopmans theorem is employed to derive crucial global reactivity parameters like chemical hardness (η), softness (S), chemical potential (μ), electronegativity (χ) and electrophilicity index (ϖ). So, according to Koopmans theorem (El-Saady et al., 2023; Limbu et al., 2024):
The molecule's hardness (η) is written as,

$$\text{Chemical hardness}(\eta) = \frac{1}{2}(\text{I-A}) \ldots\ldots\ldots (3)$$

The reciprocal of hardness is the molecule's softness and is

$$\text{Softness}(S) = \frac{1}{\eta} \quad \ldots\ldots\ldots\ldots\ldots (4)$$

The molecule's chemical potential (μ) is the opposite of its hardness and this

$$\text{Chemical potential}(\mu) = -\frac{1}{2}(\text{I+A}) \ldots\ldots (5)$$

A measure of an atom's capacity to draw electrons into a chemical bond is called electronegativity and the equation for the molecule's electronegativity (χ) is given by

$$\text{Electronegativity}(\chi) = \frac{1}{2}(\text{I+A}) \ldots\ldots\ldots (6)$$

The molecule's electrophilicity index (ω) is

$$\text{Electrophilicity}(\omega) = \frac{\mu^2}{(2\eta)} \ldots\ldots\ldots\ldots (7)$$

This study was conducted in the lowlands of the Jhapa district in the vicinities of the Kankai river. The study area was divided into six sampling stations based on the purposive sampling method starting from Domukha in the

north to Kachhudaha in the south and covering a length of 12 km. Each sampling station was subdivided into 10 grids each measuring 50m x 50m.

3. RESULT AND DISCUSSION

3.1 Optimized Molecular Geometry

The optimization energy of a molecule refers to the energy needed for it to reach its most stable and neutral state (Rai et al., 2021). Figure 2 displays the optimized geometry of the trichloroacetaldehyde molecule together with their atoms labelled by numbering and symbols. In Figure 2, the grey color represents the carbon atom, red color represents the oxygen atom and green color shows the chlorine atom where the remaining white one shows the hydrogen atom.

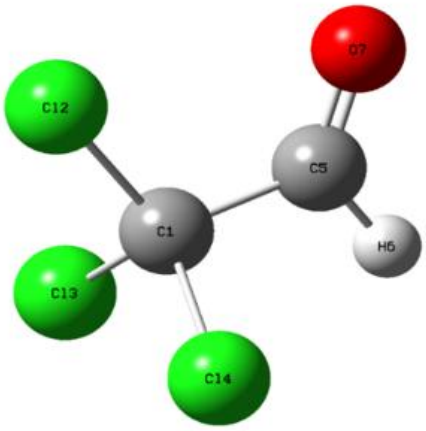

Figure 2
Optimized structure of trichloroacetaldehyde with numbering of atoms and their symbols

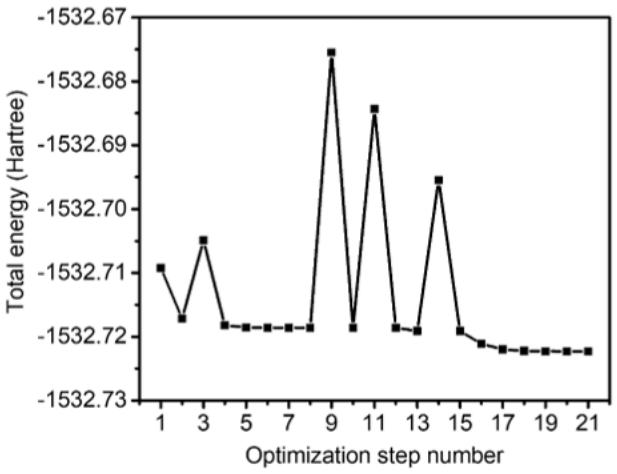

Figure 3
Total energy with respect to optimization step number

Figure 3 shows the graph of optimized total energy vs total steps number of trichloroacetaldehyde molecule. It is seen that the entire optimization phenomenon takes place in 21 different steps to set stable energy configuration. The trichloroacetaldehyde molecule's optimization energy in the gas phase was found to be -41707.52 eV (i.e. -1532.72 Hartree) along with its dipole moment 1.57 Debye. The 21 number of optimization steps and the rise and fall of the optimization energy shows the complex arrangement and geometry of the atoms in the molecule to come at its stable state.

During the optimization, the precise coordinates of every atom in the molecule's structure get updated by spatial arrangement defining the bond lengths, bond angles and dihedral angles. The energy gradients provide the forces occurring on each atom, which shows the direction and strength of the modifications required to achieve a stable configuration.

3.2 Vibration Analysis

The trichloroacetaldehyde molecule is composed of 7 atoms having 15 modes of vibration. Generally, molecule shows two types of vibration, they are stretching modes of vibration (symmetric and asymmetric stretching vibration) and deformation of bending vibration (in-plane and out-of-plane vibration). Further, in-plane vibration is divided into scissoring and rocking vibration and out-of-plane vibration is divided into twisting and wagging vibration (Budha et al., 2024; Ojha et al. 2023).

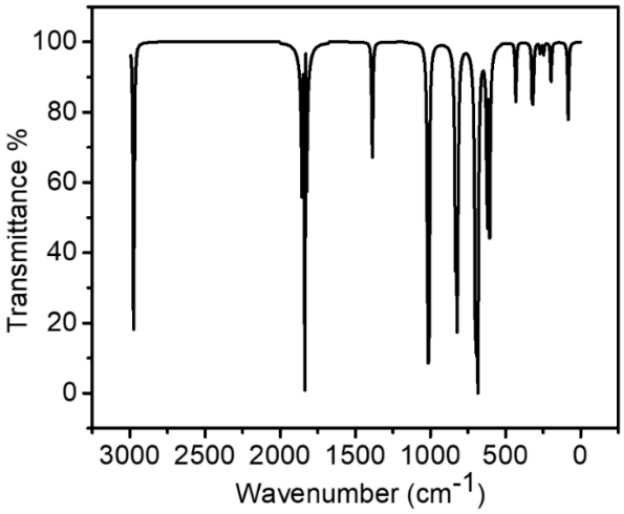

Figure 4
FT-IR spectra of trichloroacetaldehyde molecule

Figure 4 shows the FT-IR transmittance spectra of various modes of vibration of the trichloroacetaldehyde molecule in the range of 0-3500 cm^{-1}. Each frequency's transmittance % on the Y-axis indicates the intensity of light absorption and X-axis value of wavenumber corresponds to the frequencies without presence of negative values inferring absence of fictitious mode of vibration. These different modes of vibrations are from the relationship between the frequency and wavelength of infrared light (transmittance or absorption) as the result of interaction of matter with infrared radiation (Wang et al., 2012; Ghimire et al., 2022; Khadka et al., 2025).

C-C vibration

Every chemical bond oscillates at a specific frequency that corresponds to a specific energy level. The oscillation frequency of each chemical bond is directly related to its

wavenumber, which is measured in units per centimeter. C–C stretching modes of vibration are anticipated to manifest in the 1625–1450 cm^{-1} range (Wang et al., 2012; Basnet et al., 2024). Figure 4 shows the C-C vibration that occurs at 1386 cm^{-1} in our trichloroacetaldehyde molecule.

C-H vibration

In C-H vibration, stretching and wagging modes of vibrations are seen above 3000 cm^{-1} and around 1000 cm^{-1} respectively (Wang et al., 2012; Ghimire et al., 2024). In our molecule, the C-H stretching mode of vibration is observed at 2974cm^{-1} (which is nearly around 3000 cm^{-1}) and wagging mode of vibrations are seen at the 1012 and 1015 cm^{-1}. Usually, the aldehyde group's C–H stretch is seen as small bands between 2700 and 2900 cm^{-1}. When there are stronger vibrations present, these peaks may be hidden or hard to see since they are not as strong as other functional group vibrations.

C=O vibration

The carbonyl group (C=O) is easily recognized in the FT-IR spectra. The range of C=O vibration stretching mode is 1643 - 1750 cm^{-1} (Wang et al., 2012; Ojha et al. 2023). In this molecule, the observed vibration peak from the Figure 4 is 1839 cm^{-1} for C=O mode. Aldehydes often create separate carbonyl bands such that the C=O stretch vibration is visible differently in trichloroacetaldehyde.

C-Cl vibration

The stretching mode of C-Cl vibrations are found in the range of 850–550 cm^{-1} (Wang et al., 2012; Ojha et al. 2023). In our molecule, the observed stretching mode of vibrations occur at 692 cm^{-1}, 825 cm^{-1} and these values agree very well with the references. Despite being defining feature of chlorinated compounds, C-Cl stretches can be difficult to identify due to their overlap across different bending modes. Due to the absence of conjugation, trichloroacetaldehyde is less prone to C=O and C=C overlap, though spectral interference from other components may still occur.

3.3 Molecular electrostatic potential (MEP), Electrostatic potential (ESP) and Electron density (ED)

The molecular electrostatic potential (MEP) at any given point surrounding a molecule reflects the overall electrostatic influence exerted by the molecule's combined charge distribution (comprising electrons and nuclei) at that specific location. This MEP correlates with various molecular properties such as dipole moments, electronegativity, partial charges and chemical reactivity, offering insight into the molecule's polarity and overall charge distribution (Limbu et al., 2024; Shin et al. 2016).

Figures 5(a) and 5(b) are the solid view and mesh view with the color grading molecular electrostatic potential following the order: red < orange < yellow < green < blue. They show the MEP surface map values ranging from -3.401e-2 a.u. (red) to 3.401e-2 a.u. (blue). In the Figures 5(a) and (b), positively charged regions are identified by blue color whereas negatively charged regions are represented by red color. Shades of red represents electron density for negative electrostatic potential while shades of blue represent atomic nuclei for positive electrostatic potential. Figure 5(c) displays projections of electrostatic potential surfaces both along the molecular plane and perpendicular to it. The electrostatic potential gradient progresses from red to orange to green to blue with its value ranging from -6.986e-3 a.u to 6.986e-3 a.u. This visualization offers insight into the chemically active sites and allows for a comparison of atom reactivity. The various electrostatic potential values are visually depicted using different colors in which red color in Figure 5(c) signifies areas with the most negative electrostatic potential, blue indicates regions with the most positive electrostatic potential, and green denotes areas with zero potential. Figure 5(d) shows the mapping electron density onto the surface with electrostatic potential allows visualization of the molecule's size, shape, charge density, and reactive sites.

The atoms interact with one another and behave chemically as a whole is greatly influenced by the charge distributions inside molecules. Dipole-dipole and ion-dipole interactions, among the various interactions, can be studied with the use of the charge distribution. It influences properties such as polarity, conductivity, solubility, and optical behavior, making it essential for applications in drug design, materials science, and nanotechnology.

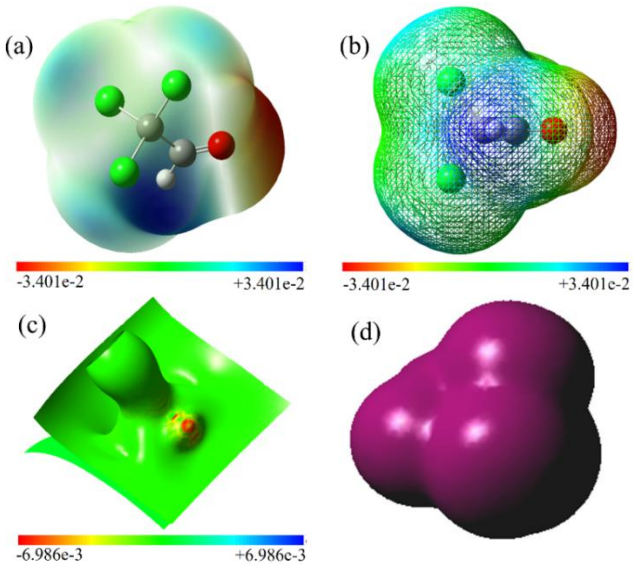

Figure 5

(a) Solid view (b) mesh view of molecular electrostatic potential (c) electrostatic potential and (d) electron density mapping of trichloroacetaldehyde

3.4 HOMO and LUMO Analysis

If the HOMO-LUMO gap is small, it implies strong reactivity towards nucleophiles or electrophiles (Ojha et al., 2023). On the other hand, a wide HOMO-LUMO gap indicates reduced chemical activity and better stability and it accounts for a molecule's survival in particular conditions. The HOMO orbital refers to the outermost (highest energy) orbital that contains electrons and its function as electron donors. The term LUMO orbital refers to the innermost (lowest energy) orbital that has the ability to accept electrons

and its function as an electron acceptor. From the frontier molecular orbital theory, an interaction between the reactants frontier orbitals (HOMO and LUMO) results in the formation of a transition state (Joshi et al., 2013; Gharti Magar et al., 2024). HOMO-LUMO energy differential has a significant stability index. It is a crucial parameter for electrical transport characteristics of molecules since it is a measure of electron conductivity. The electronic transition is higher with lower energy gap value and vice versa. Figure 6 shows the HOMO-LUMO plot with the orbital energy of -8.47 eV and - 2.48 eV respectively such that the energy differential gap of 5.99 eV is found in the trichloroacetaldehyde molecule. High HOMO-LUMO gap compounds are relatively tougher. Numerous applications in material science, including the investigation of catalytic electronic characteristics (Khadka et al. 2023), both the reactivity and stability of polymers are determined by the HOMO-LUMO gap.

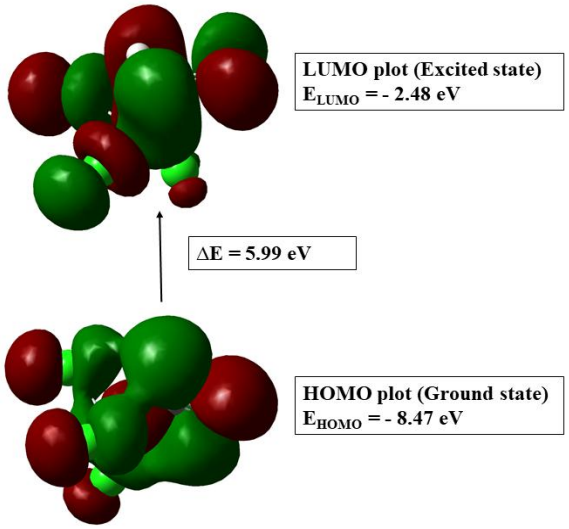

Figure 6
Plot of HOMO-LUMO and their energy gap

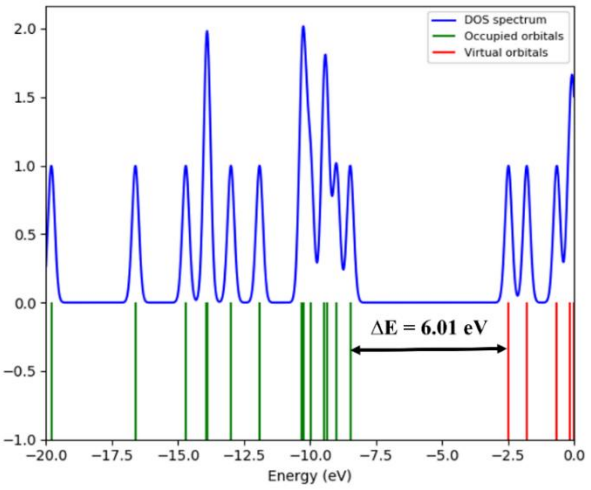

Figure 7
Density of states (DOS) plot of trichloroacetaldehyde molecule.

3.5 Density of States (DOS)

Density of states (DOS) allow us to stimulate electrons moving from the valence band into the conduction band. The DOS spectra in Figure 7 provides the availability of numerous states at various levels of the trichloroacetaldehyde molecule. In this case, positive value denotes a bonding relationship, negative value indicates an anti-bonding interaction and a zero value indicates none at all (Limbu et al., 2024). The negative zone, where the oxygen atom is primarily surrounded, is indicated by the red area in Figure 7. The positive zone of the title molecules is similarly represented by various color (blue color and shades of blue color) regions with the largest dominating area. Figure 7 shows that trichloroacetaldehyde molecule has 6.01 eV energy which is very much close to energy gap (5.99 eV) obtained from HOMO-LUMO gap of trichloroacetaldehyde.

3.6 Global Reactivity Parameters

The trichloroacetaldehyde molecule's global reactivity indices include ionisation potential (I), electron affinity (A), hardness (η), softness (S), chemical potential (μ), electronegativity (χ), electrophilicity index (ω), and. The smallest amount of energy needed to remove an electron from an atom or molecule in its gaseous state to infinity is known as the ionisation energy (I). Conversely, the energy released when an electron is added to a neutral atom or molecule to generate a negative ion in the gaseous state is known as electron affinity (A) (El-Saady et al., 2023; Rai et al., 2018). HOMO and LUMO orbitals are connected to ionization potential (I) and electron affinity (A), with the negative of the HOMO and LUMO energies corresponding to the ionization potential (I) and electron affinity (A) respectively (El-Saady et al., 2023). So we get that the I and A are 8.47 eV and 2.48 eV respectively. The calculated global hardness (η) of trichloroacetaldehyde molecule is 2.99 eV and it indicates the molecule's stability and resistance to change or deform their lowest or the occupied orbital state which can also be called its electronic configuration due to chemical reaction. The inverse of the hardness is softness (S) and its value is 0.33 eV^{-1}. It means its polarizability and ease of electron transfer or ability of a molecule to donate or take electrons with ease. Chemical potential (μ) is a measure of a substance's potential energy. A molecule that has a higher negative chemical potential is more likely to react or release energy and its value is -5.47 eV. Electronegativity (χ), calculated as 5.47 eV, indicates the molecule's electron-attracting ability. This higher and positive value obtained indicates the strong tendency to attract the electrons. The global electrophilicity index (ω) with the value 5.00 eV indicates the tendency of an atom or a molecule to accept an electron in a chemical reaction aiding in predicting its reactivity toward nucleophiles in chemical processes. If the electrophilicity index (ω) is more than 1.5 eV, it is considered strong; if it is between 0.8 and 1.5 eV, it is said to be moderate and if it is less than 0.8 eV, it is assumed marginal (Akman et al., 2023).

3.7 Mulliken Atomic Charges

One of the most popular population analyses for dividing an electron density or evolving wave function into bond orders is the Mulliken atomic charges analysis. The impact of atomic displacement on electronic structure is explained by Mulliken atomic charge. In process of electronegativity equalization, it describes charge transfer (Rai et al., 2024). Figure 8 with the analysis shows that the C1 atom exhibits highest positive charge while C5 atom exhibits highest negative charge. In addition, all chlorine atoms i.e. Cl2, Cl3 and Cl4 along with O7 atom also exhibit negative charge. For C1 and H6, the dual descriptor values seemed to be positive, indicating that they are susceptible to a nucleophilic attack. Because of their ability to accept charge, the hydrogen atom exhibits a net positive charge associated with the carbon as seen in the charge distribution. On the other hand, Cl2, Cl3, Cl4, C5, and O7 have negative values, indicating that they are susceptible to an electrophilic attack on the negative side. It is found that the negative charges on the chlorine atoms are due to their electron withdrawing and donating nature (Fayed et al., 2020; Rai et al., 2024; Ahn et al., 2018). The partial charges on the atoms within a molecule are reflected in Mulliken charges, which affect dipole-dipole interactions, van der Waals forces, and hydrogen bonds, among various intermolecular interactions.

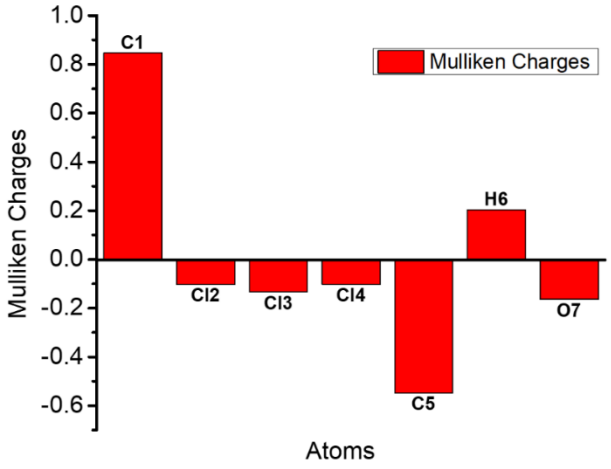

Figure 8
Histogram of calculated Mulliken charges

3.8 Thermodynamic Properties

Thermodynamic properties are examined through thermodynamic parameters, and significant changes in its structure are observed corresponding to variations in temperature (Ignatov, 2015; Rana Magar et al., 2024). The effect of temperature on thermodynamic functions, including heat capacity at constant volume (C_V), heat capacity at constant pressure (C_P), internal energy (U), enthalpy (H), entropy (S), and Gibbs free energy (G) are calculated using Moltran software.

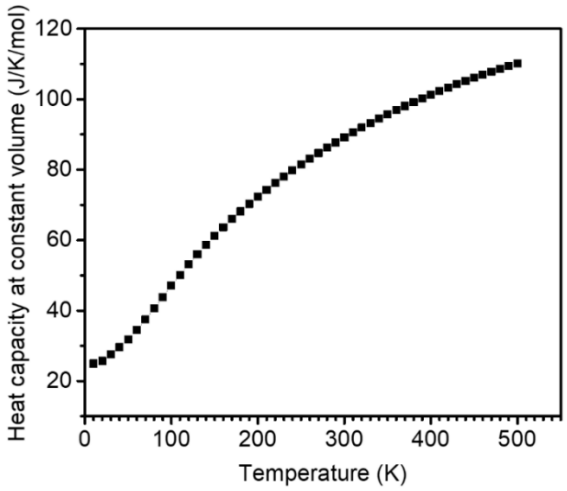

Figure 9
Temperature dependence of heat capacity at constant volume (C_V)

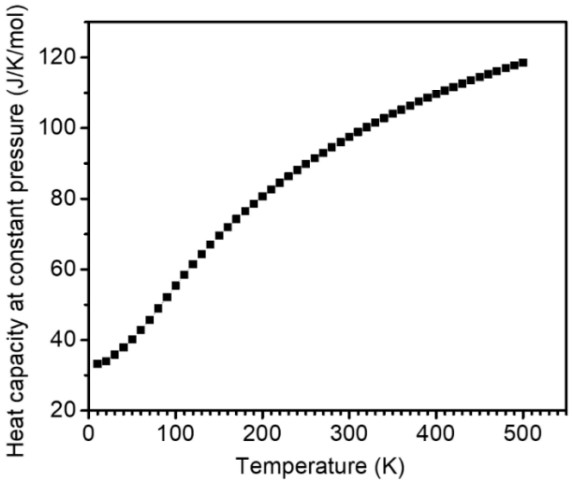

Figure 10
Temperature vs of heat capacity at constant pressure (C_P)

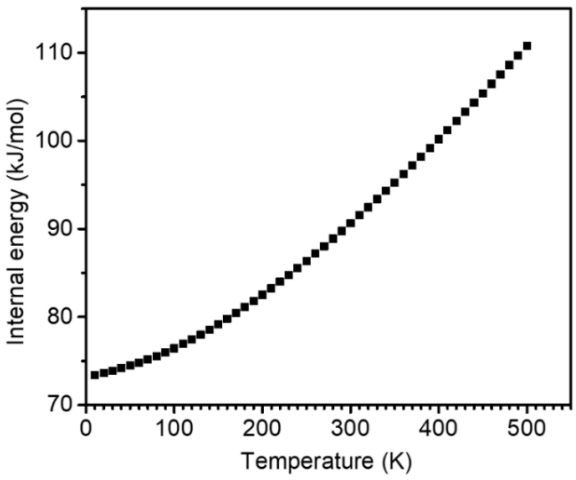

Figure 11
Temperature dependence of internal energy (U)

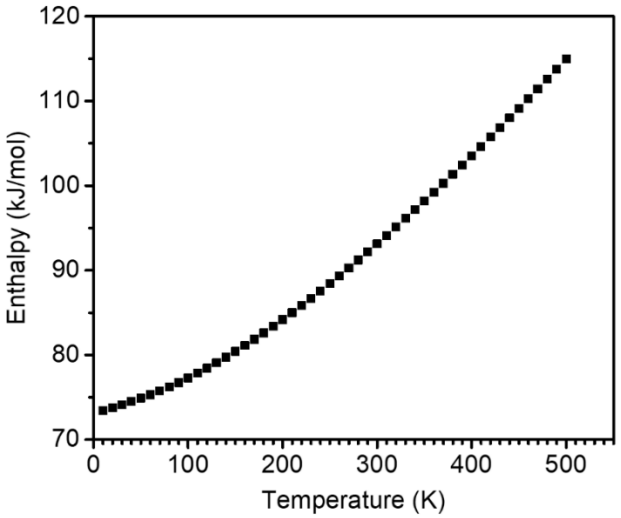

Figure 12
Temperature dependence of enthalpy (H)

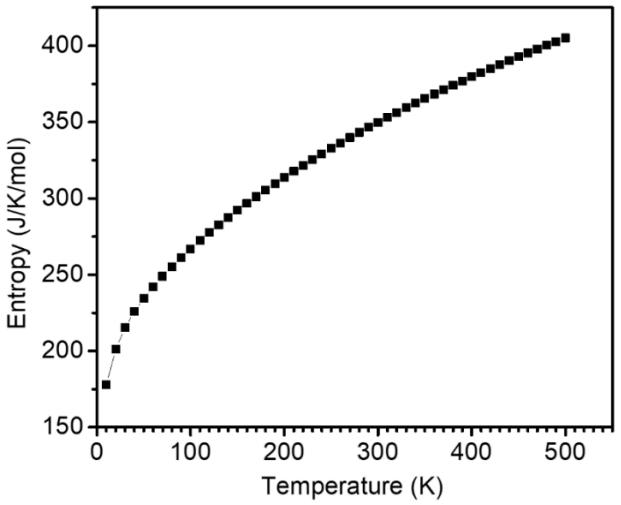

Figure 13
Temperature dependence of entropy (S) of trichloroacetaldehyde

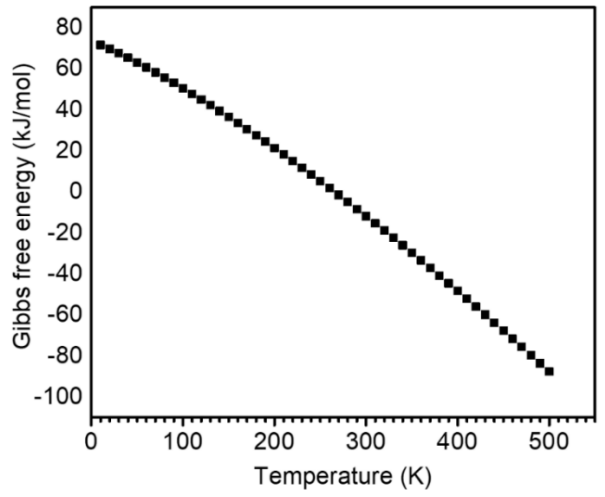

Figure 14
Temperature dependence of Gibbs Free Energy (G) of trichloroacetaldehyde

Figure 9 shows a progressive increase of energy in between the temperature of 30 to 150 K. However, after that, there is a small deviation in the rate at which heat capacity at constant volume increases as temperature rises.

Figure 10 shows that as temperature rises, so does the heat capacity at constant pressure. Up to the temperature in between 30 to 150 K, the rate of rise of heat capacity at constant pressure (C_P) is gradually more. But beyond that, there is a slight decrease in the rate of heat capacity that increases with the rise in temperature.

Figure 11 depicts the temperature relationship with the internal energy of trichloroacetaldehyde molecule. It shows the title molecule's total internal energy (U) rises with rise in temperature. Within 10 to 70 K temperature range, internal energy values increase gradually and beyond that range, the curve's nature indicates a rapidly increasing rate of internal energy values with rise in temperature

Figure 12 shows that the molecules' enthalpy increases gradually as temperature rises, indicating that the title molecule is more flexible in adjusting their own thermodynamic system in reaction to the rise in temperature.

Figure 13 shows that the entropy of the molecule increases with rise in temperature. There is a rapid increase in entropy up to the temperature 40 K. However, beyond the temperature of 40 K, the entropy values grow gradually.

Figure 14 illustrates how the trichloroacetaldehyde molecule's Gibbs free energy steeply drops with rise in temperature. This might be the result of Gibbs free energy having a negative overall value when entropy exceeds enthalpy. An increase in temperature causes entropy terms to become more prevalent, which lowers Gibbs free energy. So, in our work, when temperature increases gradually from 10-500 K, thermodynamic parameters like heat capacity at constant volume (C_v) and heat capacity at constant pressure (C_p), internal energy (U), enthalpy (H) and entropy (S) increase except Gibb's free energy, since molecular vibrational intensities increase with the rise in temperature (Limbu et al., 2024).

The patterns or behaviors of thermodynamic parameters in various systems or situations are different as thermodynamic trends. Temperature, a crucial factor in influencing a system's response, has a significant impact on these thermodynamic tendencies.

4. CONCLUSION

The chemical molecule trichloroacetaldehyde, sometimes referred to as chloral, has a chemical structure of Cl_3CCHO. This derivative of acetaldehyde has three chlorine atoms in place of the methyl group's three hydrogen atoms. This research found the structure, vibrational properties, electronic structures and thermodynamic properties of the trichloroacetaldehyde molecule. For the optimized structure, the title molecule went through twenty-one optimization step. Trichloroacetaldehyde with a neutral charge has spectra of wagging mode of vibration at about 1000 cm^{-1}. The C–C stretching modes of vibration are between 1625 and 1450 cm^{-1} and the C–H stretching modes of vibration are above 3000 cm^{-1}. On the other hand, the C-Cl stretching vibrations mode is detected between 850-550 cm^{-1}, whilst the C=O vibration stretching mode exhibits a variety of

vibration bands between 1643-1700 cm^{-1}. The arrangement of charge distribution within the molecule was revealed by ESP, MEP and ED analysis. The energy differences of 6.01 eV determined by DOS calculation is nearly identical to the 5.99 eV obtained by HOMO and LUMO analysis. It has been found that the values of the global parameters i.e. hardness, softness, chemical potential, electronegativity, and electrophilicity index are 2.99 eV, 0.33 eV^{-1}, -5.47 eV, 5.47 eV and 5.00 eV, respectively. Mulliken charges analysis of the trichloroacetaldehyde molecule show that the Cl2, Cl3, Cl4, C5 and O7 correspond to negative charges, whereas the C1 along with H6 atom correlate to positive charges. This molecule's thermodynamic analysis demonstrates that, with the exception of the Gibbs free energy, its heat capacity at constant volume, heat capacity at constant pressure, internal energy, enthalpy and entropy all increase with temperature. Considering all these things, this research advances science in a number of areas, including photochemistry, molecular docking and the examination of infrared absorption properties to assess its potential as greenhouse gas. It also aids in hydration reactions and solvent research. It is beneficial to look into possible metal catalyst or complex routes in organic chemistry. This study allows us to compare the characteristics and reactivity of other halogenated aldehydes.

ACKNOWLEDGEMENTS

The authors are very much thankful to the Department of Physics, Patan Multiple Campus, Tribhuvan University and Department of Physics, St. Xavier's College, Kathmandu, Nepal.

CONFLICTS OF INTEREST

The authors report no conflicts of interest for this research work.

REFERENCES

Abbas, R. & Fisher, J. W. (1997). A physiologically based pharmacokinetic model for trichloroethylene and its metabolites, chloral hydrate, trichloroacetate, dichloroacetate, trichloroethanol, and trichloroethanol glucuronide in B6C3F1 mice. *Toxicology and applied pharmacology*, 147(1), 15–30. https://doi.org/10.1006/taap.1997.8190

Ahn, S. J., Kim, H. W., Khadka, I. B., Rai, K. B. & Ahn, J. R. (2018). Electronic Structure of Graphene Grown on a Hydrogen-terminated Ge (110) Wafer. *Journal of Korean Physical Society*, 73(5): 656–660. https://doi.org/10.3938/jkps.73.656

Akman, F., Demirpolat, A., Kazachenko, A. S., Kazachenko, A. S., Issaoui, N. & Al-Dossary, O. (2023). Molecular structure, electronic properties, reactivity (ELF, LOL, and Fukui), and NCI-RDG studies of the binary mixture of water and essential oil of phlomis Bruguieri. *Molecules*, 28(6), 2684. https://doi.org/10.3390/molecules28062684

Barrott, L. (2004). Chloral hydrate: formation and removal by drinking water treatment. *Journal of Water Supply: Research and Technology AQUA*, 53(6), 381-390. https://doi.org/10.2166/aqua.2004.0030

Basnet, K., Neupane, B., Gharti Magar, P., Uprety, R. & Rai, K. B. (2024). A Computational DFT Insight into the Optimized Structure, Electronic Structures, Spectroscopic Analysis, and Thermodynamic Parameters of the Cytosine Molecule. *Amrit Research Journal*, 5(1), 140–150. https://doi.org/10.3126/arj.v5i1.73566

Becke, A. D. (1996). Density-functional thermochemistry. In *Book of Abstracts, 212th ACS National Meeting, Orlando, FL,* August 25–29.

Budha, C. & Rai, K. B. (2024). Study of the Molecular Structure, Spectroscopic Analysis, Electronic Structures and Thermodynamic Properties of Niacin Molecule Using First-principles. *Journal of Nepal Chemical Society*, 44(2), 1–12. https://doi.org/10.3126/jncs.v44i2.68263

Edwards, P. M. (2002). Origin 9.0: scientific graphing and data analysis software. *Journal of chemical information and computer sciences*, *42*(5), 1270–1271.

El-Saady, A. A., Roushdy, N., Farag, A. A. M., El-Nahass, M. M. & Abdel Basset, D. M. (2023). Exploring the molecular spectroscopic and electronic characterization of nanocrystalline Metal-free phthalocyanine: a DFT investigation. *Optical and Quantum Electronics*, 55(7), 662. https://doi.org/10.1007/s11082-023-04877-8

Fayed, T. A., Gaber, M., El-Nahass, M. N., Diab, H. A. & El-Gamil, M. M. (2020). Synthesis, Structural characterization, thermal, molecular modeling and biological studies of chalcone and Cr (III), Mn (II), Cu (II) Zn (II) and Cd (II) chelates. *Journal of Molecular Structure*, 1221, 128742. https://doi.org/10.1016/j.molstruc.2020.128742

Frisch, A. J. H. A., Nielson, A. B. & Holder, A. J. (2000). Gaussview user manual. *Gaussian Inc., Pittsburgh, PA*, *556*. Frisch, M. J. Gaussian 09, Revision D. 01/Gaussian (2009)

Gaus, H., Olsen, P., Van Sooy, K., Rentel, C., Turney, B., Walker, K. L., McArdle, J. V. & Capaldi, D. C. (2005). Trichloroacetaldehyde modified oligonucleotides. *Bioorganic & medicinal chemistry letters*, 15(18), 4118–4124. https://doi.org/10.1016/j.bmcl.2005.06.018

Gharti Magar, P., Uprety, R. & Rai, K. B. (2024). First-Principles DFT Study of the Molecular Structure, Spectroscopic Analysis, Electronic Structures and Thermodynamic Properties of Ascorbic Acid. *Himalayan Physics*, 11(1), 28–40. https://doi.org/10.3126/hp.v11i1.65329

Ghimire, R., Magar, A. R., Basnet, B., Uprety, R., Pudasainee, K. & Rai, K. B. (2024). Study of the Spectroscopic Analysis, Electronic Structure and Thermodynamic Properties of Ethyl benzene Using First-Principles Density Functional Theory. *Contemporary Research: An Interdisciplinary Academic Journal*, 7(1), 80–99. https://doi.org/10.3126/craiaj.v7i1.67259

Ghimire, R. R., Parajuli, A., Gupta, S. P. & Rai, K. B. (2022). Synthesis of ZnO Nanoparticles by Chemical Method and its Structural and Optical Characterization. *BIBECHANA*, 19(1-2), 90–96. https://doi.org/10.3126/bibechana.v19i1-2.46396

Gordeev, A. D., Efremov, D. I., Soifer, G. B. & Shchepin, V. V. (1996). Quantum chemical calculations and35Cl NQR study of the molecular structure of trichloroacetyl halides and trichloroacetaldehyde. *Journal of structural chemistry*, 37(3), 431–436. https://doi.org/10.1007/BF02578596

Ignatov, S. K. (2015). Moltran v. 2.5-Program for molecular visualization and thermodynamic calculations. *University of Nizhny Novgorod*.

Joshi, B. D., Tandon, P. & Jain, S. (2013). Structure, MESP and HOMO-LUMO study of 10-Acetyl-10H-phenothiazine 5-oxide using vibrational spectroscopy and quantum chemical methods. *BIBECHANA*, 9, 38–49. https://doi.org/10.3126/bibechana.v9i0.7151

Khadka, I. B., Rai, K. B., Alsardia, M. M., Haq, B. U. & Kim, S. H. (2023). Raman investigation of substrate-induced strain in epitaxially grown graphene on low/high miscut angled silicon carbide and its application perspectives, *Optical Materials*, 140, 113836. https://doi.org/10.1016/j.optmat.2023.113836

Khadka, I. B., Rai, K. B. & Rokka, D. (2025). Low-power light irradiation based plasmonic photoresponse on quasi-freestanding monolayer/AuNPs hybrid system. *Indian Journal of Physics,* 99(1), 95–103. doi.org/10.1007/s12648-024-03254-9

Li, H., Sun, W., Deng, M., Zhou, Q., Wang, J., Liu, J. & Zhang, Y. (2018). Asperversiamides, linearly fused prenylated indole alkaloids from the marine-derived fungus Aspergillus versicolor. *The Journal of Organic Chemistry*, 83(15), 8483–8492. http://dx.doi.org/10.1021/acs.joc.8b01087

Limbu, S., Ojha, T., Ghimire, R. R. & Rai, K. B. (2024). An investigation of vibrational analysis, thermodynamics properties and electronic properties of Formaldehyde and its stretch by substituent acetone, acetyl chloride and methyl acetate using first principles analysis. *BIBECHANA*, 21(1), 23–36. https://doi.org/10.3126/bibechana.v21i1.58684

Luknitskii, F. I. (1975). Chemistry of chloral. *Chemical Reviews*, 75(3), 259–289. https://doi.org/10.1021/cr60295a001

Neupane, R., Gauli, H. R. K. & Rai, K. B. (2022). Average Intensity and Wavelength of the Emitted Radiations from Earth Surface with Error Analysis. *Nepal Journal of Science and Technology*, 21(2), 29–46. https://doi.org/10.3126/njst.v21i2.62354

Nolan, L., Kelly, T., Wenger, J., Treacy, J., Wirtz, K. & Sidebottom, H. (2002). The photochemical degradation of chloral and oxalyl chloride. In I. Barnes (Eds.), Global Atmospheric Change and its Impact on Regional Air Quality, (pp. 97-101). NATO Science Series, vol 16. Springer, Dordrecht. https://doi.org/10.1007/978-94-010-0082-6_15

Ojha, T., Limbu, S., Shrestha, P. M., Gupta, S. P. & Rai, K. B. (2023). Comparative Computational Study on Molecular Structure, Electronic and Vibrational Analysis of Vinyl Bromide based on HF and DFT Approach. *Himalayan Journal of Science and Technology*, 7(1), 38–49. https://doi.org/10.3126/hijost.v7i1.61128

O'Nolan, D., Perry, M. L. & Zaworotko, M. J. (2016). Chloral hydrate polymorphs and cocrystal revisited: solving two pharmaceutical cold cases. *Crystal Growth & Design*, 16(4), 2211–2217. https://doi.org/10.1021/acs.cgd.6b00032

Rai, K. B., Ghimire, R. R., Dhakal, C., Pudasainee, K. & Siwakoti, B. (2024). Structural Equilibrium Configuration of Benzene and Aniline: A First-Principles Study, *Journal of Nepal Chemical Society*, 44(1), 1–15. doi.org/10.3126/jncs.v44i1.62675

Rai, K. B., Khadka, I. B., Kim, E. H., Ahn, S. J., Kim, H. W. & Ahn, J. R. (2018). Influence of Hydrophobicity on the Chemical Treatments of Graphene. *Journal of Korean Physical Sociey,* 72(1): 107–110. https://doi.org/10.3938/jkps.72.107

Rai, K. B., Khadka, I. B., Koirala, A. R. & Ray, S. C. (2021). Insight of cleaning, doping and defective effects on the graphene surface by using methanol. *Advances in Materials Research,* 10(4), 283–292. https://doi.org/10.12989/amr.2021.10.4.283

Rai, K. B., Teemilsina, N. K. & Siwakoti, B. (2024). First principles study of structural equilibrium configuration of Ortho-, Meta-, and Para-chloroaniline molecules. *Scientific World*, 17(17), 7–18. https://doi.org/10.3126/sw.v17i17.66414

Magar, A. R., Ghimire, R., Basnet, B., Shrestha, P. M., Gupta, S. P. & Rai, K.B. (2024). First-principles Calculation of Cumene: Molecular Structure, Electronic Structures, Spectroscopic Analysis, and Thermodynamic Properties. *Molung Educational Frontier*, 14(1), 1–26. https://doi.org/10.3126/mef.v14i01.67890

Rajendram, R., Rajendram, R. & Preedy, V. R. (2016). Acetaldehyde: A Reactive Metabolite. In V. R. Preedy (Eds.), *Neuropathology of Drug Addictions and Substance Misuse* (pp. 552–562). Academic Press. https://doi.org/10.1016/B978-0-12-800213-1.00051-1

Shin, H. C., Ahn, S. J., Kim, H. W., Moon, Y., Rai, K. B., Woo, S. H. & Ahn, J. R. (2016). Room temperature deintercalation of alkali metal atoms from epitaxial graphene by formation of charge-transfer complexes. *Applied Physics Letters,* 109(8), 081603. Doi:10.1063/1.4961633

Wang, J., Qiu, X., Wang, Y., Zhang, S. & Zhang, B. (2012). Vibrational Spectra and Quantum Calculations of Ethylbenzene. *Chinese Journal of Chemical Physics,* 25(5), 526–532. DOI:10.1088/1674-0068/25/05/526-532